

# Efficiency of heat recovery versus maximum catalyst temperature in a reverse-flow combustion of methane

Krzysztof Gosiewski

*Institute of Chemistry and Environmental Protection, Jan Dlugosz University of Czestochowa,  
ul. Armii Krajowej 13/15, 42-201 Czestochowa, Poland*

## Abstract

Results of simulations are presented concerning a reverse-flow reactor for the catalytic combustion of methane that occurs in coal-mine ventilation air. The simulations were performed for two types of catalyst: 12%  $\text{MnO}_2/\gamma\text{-Al}_2\text{O}_3$  and 0.5%  $\text{Pd}/\gamma\text{-Al}_2\text{O}_3$ . A special attention is given to maximum temperature of the catalyst bed in order to minimize occurrence of homogeneous combustion. The simulations revealed that there is a visible contradiction between efficiency of heat recovery aimed to high-pressure steam production and efforts to constraint maximum temperature in the bed.

© 2004 Elsevier B.V. All rights reserved.

*Keywords:* Chemical reactors; Combustion; Dynamic simulation; Heat recovery; Mathematical modeling; Reverse-flow reactors

## 1. Introduction

Methane has global warming potential (GWP) several times higher than that of  $\text{CO}_2$ . Furthermore, it is emitted from a host of sources and thus produces a substantial contribution to overall global warming (the estimated share of  $\text{CH}_4$  is around 19%). Large quantities of methane are exhausted to the atmosphere with coal-mine ventilation air with very low  $\text{CH}_4$  content (0.1–1 vol.%). The global emission of methane from this source is estimated at, roughly, 15 Mt/year. Apart from the environmental impact this leads to considerable energy losses, as methane is a fuel in its own right. Unfortunately, the concentration of methane in ventilation air is too low to support homogeneous combustion. Thus, the only viable option is catalytic oxidation in an autothermal reverse-flow reactor fitted with an energy withdrawal system to recover the heat from the hottest parts of the catalytic bed.

Reverse-flow reactors have been increasingly used in practice, especially in catalytic oxidation of the various compounds that produce too little heat to sustain autothermicity in a traditional stationary reactor, and also, in processes in which

the efficient recovery of the heat of exothermal reactions is of crucial importance. The relevant literature is abundant; we shall mention here the fundamental monograph of Matros [1] or, e.g. paper [2], which provide both the description, theoretical background and applications of the concept of flow-reversal reactors. The idea of the reverse-flow combustion of lean methane/air gas mixtures is also not new, since it was reported by Gogin et al. [3]. Extensive studies of reverse-flow reactor application for the oxidation of lean methane emissions from the coal-mine vent gas are recently also carried out in CANMET (Natural Resources Canada) and were reported by Sapoundijev et al. [4]. Investigations of reverse-flow lean methane catalytic combustion were lately also intensively carried out in the Boreskov Institute of Catalysis (BIC) in Novosibirsk.

Due to complex catalytic processes under unsteady-state conditions, the usual method for analyzing reverse-flow processes is based on extensive simulations using an appropriate mathematical model. There are a number of simulation techniques available (well classified by Unger et al. [5]); the most natural approach seems to be that based on successive solution of partial differential equations which describe the mass and energy balances, starting from a certain initial state up to a moment when the process in the subsequent cycles of

*E-mail address:* k.gosiewski@ajd.czyst.pl.

## Nomenclature

$c_k$	heat capacity of the catalyst ( $\text{J kg}^{-1} \text{K}^{-1}$ )
$c_{p,g}$	heat capacity of the gas ( $\text{J mol}^{-1} \text{K}^{-1}$ )
$C_{\text{CH}_4}$	methane concentration ( $\text{mol m}^{-3}$ )
$d_p$	equivalent diameter of pellet (m)
$D_e$	effective diffusion coefficient ( $\text{m}^2 \text{s}^{-1}$ )
$D_{\text{eff}}$	effective mass dispersion coefficient ( $\text{m}^2 \text{s}^{-1}$ )
$D_r$	reactor diameter (m)
$E_a$	activation energy ( $\text{J mol}^{-1}$ )
$h_{\text{surr}}$	overall heat transfer coefficient ( $\text{W m}^{-2} \text{K}^{-1}$ )
$\Delta H$	heat of reaction ( $\text{J mol}^{-1}$ )
$k_{\text{CH}_4}$	pre-exponential factor in the rate equation ( $\text{s}^{-1}$ )
$L_{\text{act}}$	thickness of the active layer of catalyst
$n_g$	molar gas flux ( $\text{mol m}^{-2} \text{s}^{-1}$ )
$Pe_g = \frac{ud_p}{D_{\text{eff}}}$	dimensionless Peclet number for mass dispersion
$r_{\text{CH}_4}$	rate of the catalytic combustion of methane ( $\text{mol kg}^{-1} \text{s}^{-1}$ )
$r_{\text{hom}}$	rate of the thermal combustion of methane ( $\text{mol m}^{-3} \text{s}^{-1}$ )
$R$	gas constant ( $\text{J mol}^{-1} \text{K}^{-1}$ )
$S$	external specific surface area of catalyst ( $\text{m}^{-1}$ )
$t$	time (s)
$T$	temperature (K)
$T_{g,\text{in}}^{\text{1st bed}}, T_{g,\text{in}}^{\text{2nd bed}}$	1st and 2nd bed inlet temperatures (K)
$T_{g,\text{out}}^{\text{1st bed}}$	1st bed outlet temperature (K)
$u$	superficial gas velocity ( $\text{m s}^{-1}$ )
$y_{\text{CH}_4}^g$	methane mole fraction in the gas phase
$y_{\text{CH}_4}^s$	methane mole fraction on the catalyst surface
$z$	axial coordinate along the bed (m)

### Greek letters

$\alpha$	heat transfer coefficient ( $\text{W m}^{-2} \text{K}^{-1}$ )
$\beta$	mass transfer coefficient ( $\text{mol m}^{-2} \text{s}^{-1}$ )
$\varepsilon$	void fraction
$\eta$	effectiveness factor of the pellet
$\lambda_{\text{eff}}$	effective thermal conductivity ( $\text{W m}^{-1} \text{K}^{-1}$ )
$\rho_b$	bulk density of the bed ( $\text{kg m}^{-3}$ )
$\rho_g$	molar gas density ( $\text{mol m}^{-3}$ )

### Subscripts and Superscripts

c	catalyst
g	gas
in	inlet
s	catalyst surface
surr	surroundings

methane catalytic combustion experiments in a pilot plant and next industrial installation were reported by Gogin et al in [7]. Reverse-flow methane combustor model was solved and also compared with experimental results by Aube and Sapoundijev [8]. The present work comprises results of some detailed mathematical simulation study, carried out in cooperation with BIC in Novosibirsk within frame of the European Union project [13], co-ordinated by the University of Stuttgart. The aim of this paper is to show that high heat recovery efficiency is a direct contradiction of low maximum catalyst temperature.

For  $\text{CH}_4$  concentrations in the feed air below 1 vol.%, the efficient heat recovery from the reactor becomes fairly complex. The average flow rate of ventilation air emitted from a single shaft is in Poland about  $700,000 \text{ m}^3(\text{STP})/\text{h}$ ; if we assume that the energy recovery remains a viable alternative as long as  $\text{CH}_4$  concentration exceeds 0.4 vol.%, the heat flux generated due to the oxidation would be almost 28 MW (and even about 70 MW at peak methane concentration of 1 vol.%). Such quantities of energy cannot be utilized as low-quality heat, and the sole practical solution is the production of high-pressure steam, which can further be used to generate electricity. Efficient heat recovery problems for lean methane combustor were studied by Gosiewski and Warmuzinski [9,10]. In order to find the efficient method of heat recovery from a reverse-flow methane combustor a number of simulations based on mathematical model of the process were performed in the quoted study. The simulations were carried out for two different types of catalyst. Initially, the catalyst examined was that based on  $\text{MnO}_2$  but it occurred, that maximum temperature approaching  $1000^\circ\text{C}$  in the catalyst bed could be dangerous for safe catalyst work. Then, in order to ensure lower maximum temperatures within the catalytic bed (and thus, additionally to avoid the homogeneous combustion in the gas phase) the other catalyst was used with palladium as an active component. The simulations are regarded as a preliminary analysis of the process. Consequently, the exact values of the parameters characterizing the steam produced are not specified (these parameters determine, in turn, steam temperatures in the various parts of the installation). However, since the boilers usually produce superheated steam at a pressure of about 4 MPa or higher, we can tentatively assume that the system should guarantee the generation of steam of at least such quality. In such a system the low-temperature section includes a water heater (economizer), while the high-temperature part incorporates a steam superheater. The evaporators operate at intermediate temperatures. The economizer is commonly fed with treated water at a temperature slightly above 373 K ( $100^\circ\text{C}$ ), although present-day boilers enable the cooling of the gas to about 333 K ( $60^\circ\text{C}$ ) by utilizing a part of the heat in the water treatment plant. The steam produced usually has a temperature of about 723 K ( $450^\circ\text{C}$ ). These assumptions result in the following conditions: incorporating the various elements of the boiler into the heat withdrawal system and, simultaneously, providing sufficiently high temperature difference between

flow reversals begins to repeat itself. As it was shown by Gosiewski [6] theoretically more efficient iterative shooting simulation methods in this case occurred to be numerically less efficient. Mathematical simulations and results of lean

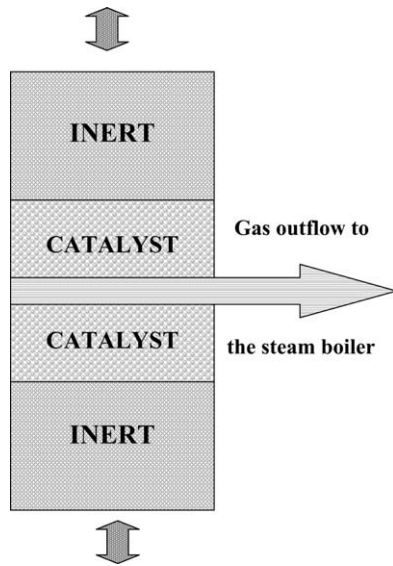


Fig. 1. Schematic diagram of the reverse-flow reactor with heat recovery by the hot gas withdrawal from the central section of the reactor.

the heating medium (gas from the reactor) and the medium that consumes heat (water and steam) requires that the gas temperature at the inlet to the boiler system should be at least 823 K (550 °C), and that the gas itself should not be cooled below 333 K (60 °C). These conditions lead to approximate temperatures characterizing the heat withdrawal system. Obviously, the higher the gas temperature at the boiler inlet the better. Too high gas temperatures in the reactor lead to yet another group of problems (among others, too large a contribution of the homogeneous combustion resulting in rapid catalyst sintering and deactivation).

## 2. Heat recovery system analyzed in the present study

In general, the heat of reaction can be withdrawn in either of the two ways. In a method termed “central cooling” the whole gas stream flows through the heat exchanger. On the other hand, the technique of “hot gas withdrawal” (Fig. 1) is based on feeding the boiler with a part of the hot gas withdrawn from the central part of the reactor, which is then discharged to the atmosphere. The simulations revealed (see [9,10]) that hot gas withdrawal would enable higher efficiency of the heat recovery than central cooling. Simulations as well as experimental study carried out in Novosibirsk’s BIC [13] revealed that up to about 30% of gas can be safely withdrawn without loss of autothermicity or stability of the process. Moreover the simulations have shown [9] that a relation exists between the method for heat withdrawal and the asymmetry in the profiles of the packed bed temperature over half-cycles of flow reversal. It was shown that central cooling promotes asymmetry of temperature profiles in the packed bed of the reactor. An increase in the amount of heat

withdrawn by central cooling of gas (by more than 120 K for the Pd catalyst or by more than 150 K for the MnO<sub>2</sub> catalyst) produces a well-marked half-cycle asymmetry, as the temperatures in one half of the reactor bed are clearly higher than those in the other half. When heat extraction further increases strongly asymmetrical cycle appears, then the reaction extinguishes. Thus in the present study only the “hot gas withdrawal” method is analyzed as this system can give higher heat recovery coefficients. A drawback of the hot gas withdrawal is that a part of the gas stream passes only through a half of the catalyst bed only, whereupon it leaves the system without participating in the reaction occurring in the second half. Effective conversion of the reactor about 90% can be obtained, however. On the other hand, the temperature of the gas withdrawn from central part is high enough that some additional fixed catalyst bed located on this side (withdrawn) stream allows obtainment of nearly full methane conversion in this stream too. So incomplete conversion is not a real problem when this solution is applied.

The amount of heat to be withdrawn from the reaction system increases with an increase in the inlet methane concentration. It is assumed that the maximum value of this concentration can reach 1 vol.%.

## 3. Mathematical model of a reverse-flow reactor

Mathematical model applied in the present study is generally the same as presented in [9,10].

### 3.1. Balance equations

The reactor is divided into two parts: Bed No. 1 (before the hot gas withdrawal) and Bed No. 2 (after the exchanger).

To facilitate the presentation of the results, the length  $z$  is measured continuously for the two beds from  $z=0$  (inlet to Bed 1) up to  $z=Z$  (outlet from Bed 2). Each bed consists of an inert section and an active section packed with catalyst. In the model, the two parts are treated as a single bed, with the exception that for the inert parts the rate of the catalytic combustion is zero in Eqs. (2) and (4), whereas for the catalytic parts the value of is calculated from an appropriate kinetic  $r_{\text{CH}_4}$  equation. The rate of the homogeneous combustion,  $r_{\text{hom}}$ , can have a non-zero value for both inert and catalytic section. In the simulations for the MnO<sub>2</sub> catalyst, because of numerical stability considerations, the contribution of the homogeneous combustion was neglected altogether.

The model comprises the following molar and energy balance equations, supplemented with the relevant initial and boundary conditions.

Energy balance for the gas :

$$0 = -n_g c_{p,g} \frac{\partial T_g}{\partial z} + \varepsilon \frac{n_g c_{p,g} d_p}{Pe_g} \frac{\partial^2 T_g}{\partial z^2} + \alpha S(T_c - T_g) - \Delta H r_{\text{hom}} \quad (1)$$

Energy balance for the catalyst :

$$\rho_b c_k \frac{\partial T_c}{\partial t} = \lambda_{\text{eff}} \frac{\partial^2 T_c}{\partial z^2} + \alpha S (T_g - T_c) + \rho_b \eta r_{\text{CH}_4} (-\Delta H) - \frac{4}{D_f} h_{\text{surr}} (T_c - T_{\text{surr}}) \quad (2)$$

Molar balance of CH<sub>4</sub> in the gas phase :

$$\varepsilon \rho_g \frac{\partial y_{\text{CH}_4}^g}{\partial t} = \varepsilon \rho_g D_{\text{eff}} \frac{\partial^2 y_{\text{CH}_4}^g}{\partial z^2} - n_g \frac{\partial y_{\text{CH}_4}^g}{\partial z} + \beta S (y_{\text{CH}_4}^s - y_{\text{CH}_4}^g) - \varepsilon r_{\text{hom}} \quad (3)$$

Algebraic equation describing mass transport from the bulk

$$\text{gastothecatalystsurface : } y_{\text{CH}_4}^s = \frac{\rho_b \eta r_{\text{CH}_4}}{\beta S} + y_{\text{CH}_4}^g \quad (4)$$

Initial conditions ( $t = 0$ ) :

$$T_c(z, 0) = T_g(z, 0) = f_1(z), \quad y_{\text{CH}_4}^g(z, 0) = f_2(z) \quad (5)$$

Boundary conditions ( $z = Z_{\text{in}}$ ) :

$$T_g(0, t) = T_{g,\text{in}} + \frac{(1 - \varepsilon)\alpha}{n_g c_{p,g}} [T_c(0, t) - T_{g,\text{in}}] + \frac{\varepsilon d_p}{Pe_g} \frac{\partial T_g}{\partial z},$$

$$\frac{\partial T_c}{\partial z} = \frac{(1 - \varepsilon)}{\lambda_{\text{eff}}} \alpha [T_c(0, t) - T_{g,\text{in}}],$$

$$\varepsilon D_{\text{eff}} \frac{1}{u} \frac{\partial y_{\text{CH}_4}^g}{\partial z} = y_{\text{CH}_4}^g(0, t) - y_{\text{CH}_4}^g(\text{in}) \quad (6)$$

where  $Z_{\text{in}} = 0$  for Bed 1 and  $Z_{\text{in}} = Z/2$  for Bed 2, and

$$z = Z_{\text{out}}, \quad \frac{\partial T_c}{\partial z} = 0, \quad \frac{\partial y_{\text{CH}_4}^g}{\partial z} = 0 \quad (7)$$

where  $Z_{\text{out}} = Z/2$  for Bed 1 and  $Z_{\text{out}} = Z$  for Bed 2.

### 3.2. Computational procedure

The equations describing the process were integrated using the PDEXIM software package [11]. The integration was carried out in two stages. First, Bed 1 (i.e. the whole section before the gas withdrawal) was integrated. Next, the flow rate for next bed was altered by the value of the hot gas outflow, and finally Bed 2 was integrated. Thus, in boundary conditions (6) the inlet temperature for the two sections is

$$\text{Bed 1 : } T_{g,\text{in}}^{1\text{st bed}} = \text{const} \quad (8)$$

$$\text{Bed 2 : } T_{g,\text{in}}^{2\text{nd bed}} = T_{g,\text{out}}^{1\text{st bed}} \quad (9)$$

The reversal of flow is modelled by restarting the calculations for the initial conditions that are a mirror copy of those corresponding to the latest moment of the preceding half-cycle.

The values of the effectiveness factor  $\eta$  that appears in Eqs. (2) and (4) were evaluated for the current point within the bed using a method described elsewhere [12]. These values were, however, modified to take into account non-isothermal conditions prevailing within the catalyst pellet. The effectiveness factor for the pellet is calculated using the linearized value of the first-order reaction rate constant:

$$\eta = \frac{\tanh \psi}{\psi}, \quad \psi = L_{\text{act}} \sqrt{\frac{k_{\text{lin}}}{D_e}} \quad (10)$$

The value of  $k_{\text{lin}}$  is evaluated using the following relation:

$$k_{\text{lin}} = \left( \frac{\partial r_{\text{CH}_4}}{\partial C_{\text{CH}_4}} \right) - (-\Delta H) \frac{D_{e,\text{CH}_4}}{\lambda_{\text{eff}}} \left( \frac{\partial r_{\text{CH}_4}}{\partial T} \right) \quad (11)$$

The simulations were performed for two types of catalyst: 12% MnO<sub>2</sub>/γ-Al<sub>2</sub>O<sub>3</sub> and 0.5% Pd/γ-Al<sub>2</sub>O<sub>3</sub>. The kinetic data were provided by the Borekov Institute of Catalysis in Novosibirsk [13]. For the manganese catalyst the necessary data were obtained based on an earlier publication of Tsyrlunikov et al. [14].

The kinetic equation used has the form

$$r_{\text{CH}_4} = k_{\text{CH}_4} \times \frac{1}{\rho_b} \times \exp\left(-\frac{E_a}{RT}\right) \times C_{\text{CH}_4} \quad (12)$$

## 4. Results of simulations

The main point of interest of simulations was the heat recovery coefficient defined as ratio of the heat recovered to the total heat produced by the methane combustion.

In Table 1 the basic input parameters are listed together with their values used in the computations. The data given in the table corresponds to a larger scale pilot plant reactor, which is planned as a next step of the research study, but quantitatively the simulated results can be extended on future industrial applications.

Simulations were carried out for manganese (12% MnO<sub>2</sub>/γ-Al<sub>2</sub>O<sub>3</sub>) and palladium (0.5% Pd/γ-Al<sub>2</sub>O<sub>3</sub>) catalyst.

Obtained by simulations heat recovery coefficient as a function of inlet methane concentration is shown in Fig. 2,

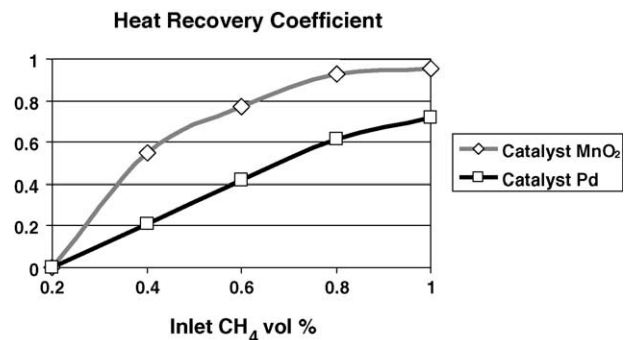


Fig. 2. Heat recovery coefficient as a function of inlet methane concentration – comparison of simulation results for MnO<sub>2</sub> and Pd catalysts.

Table 1  
Basic parameter values used in the calculations

Quantity	Value
Gas flow rate	30000 m <sup>3</sup> (STP)/h
Inlet temperature	293.15 K (20 °C)
Mole fraction of methane in ventilation air	0.01
Height of the catalyst bed	
(a) Rings 10 mm × 10 mm × 5 mm (12% MnO <sub>2</sub> /γ-Al <sub>2</sub> O <sub>3</sub> )	2 m × 0.2 m
(b) Rings 15 mm × 15 mm × 9 mm (0.5% Pd/γ-Al <sub>2</sub> O <sub>3</sub> )	
Height of the inert bed	
(a) Ceramic rings 15 mm × 15 mm × 9 mm	2 m × 0.2 m
(b) Ceramic rings 25 mm × 25 mm × 19 mm	
Superficial velocity in the reactor (at standard temperature and pressure) (m/s)	(a) 0.6 and (b) 0.4
Reactor diameter (m)	(a) 4.2 and (b) 5.144
Duration of the half-cycle of flow reversal (s)	(a) 120 and (b) 300 s

(a) Reactor with MnO<sub>2</sub> catalyst, (b) Reactor with Pd catalyst.

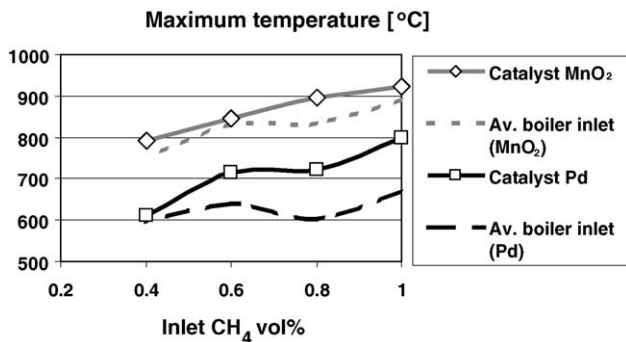


Fig. 3. Maximum temperature in the bed as a function of inlet methane concentration – comparison of simulation results for MnO<sub>2</sub> and Pd catalysts.

while in Fig. 3 the similar plot of maximum temperature in the bed. Flux of recovered heat as a function of concentration is presented in Fig. 4. Moreover, Fig. 5 presents similar comparison of the effective conversion which is feasible in the reactor. “Effective” means that the conversion was calculated regarding both gas streams, i.e. either that fully converted flowing through both reactor beds or the stream withdrawn from central part (which can be only partially converted).

For MnO<sub>2</sub> catalyst one gets either higher efficiency of heat recovery or higher maximum temperature in the reactor. Thus

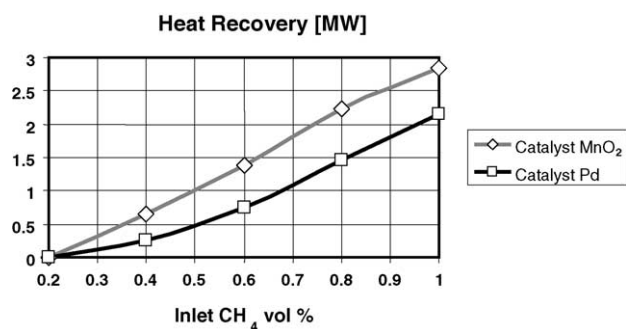


Fig. 4. Flux of recovered heat as a function of inlet methane concentration – comparison of simulation results for MnO<sub>2</sub> and Pd catalysts.

the simulations revealed that there is a visible contradiction between efficiency of heat recovery aimed to high-pressure steam production and efforts to constrain maximum temperature in the bed.

There is different methane concentration range in ventilation gas of various coal mines, dependent on region, exploitation technology, as well as on some other factors. But assuming that average vent air methane concentration is about 0.5 vol.%, it could be estimated that when applying Pd catalyst we get the 0.5 MW lower heat flux recovered, than for the case when MnO<sub>2</sub> catalyst was used. On the other hand, for the manganese catalyst, maximum temperature can exceed 900 °C when concentration approaches to 1 vol.%. Such temperature can either promote homogeneous combustion which is difficult to control or damage the catalyst. Thus in spite of much lower efficiency of heat recovery using palladium catalyst seems to be right solution.

Some more detailed simulation results obtained for Pd catalyst are presented in Figs. 6–8. The results concern stabilized cyclic steady states of the reactor for which averaged difference between temperature profiles of consecutive full reversal cycles varied from case to case within the range 0.5 to less than 0.001 K. This state has usually been achieved after

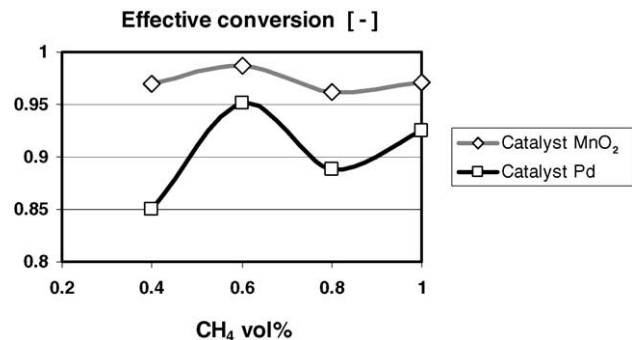


Fig. 5. Effective conversion of catalytic combustion as a function of inlet methane concentration – comparison of simulation results for MnO<sub>2</sub> and Pd catalysts.



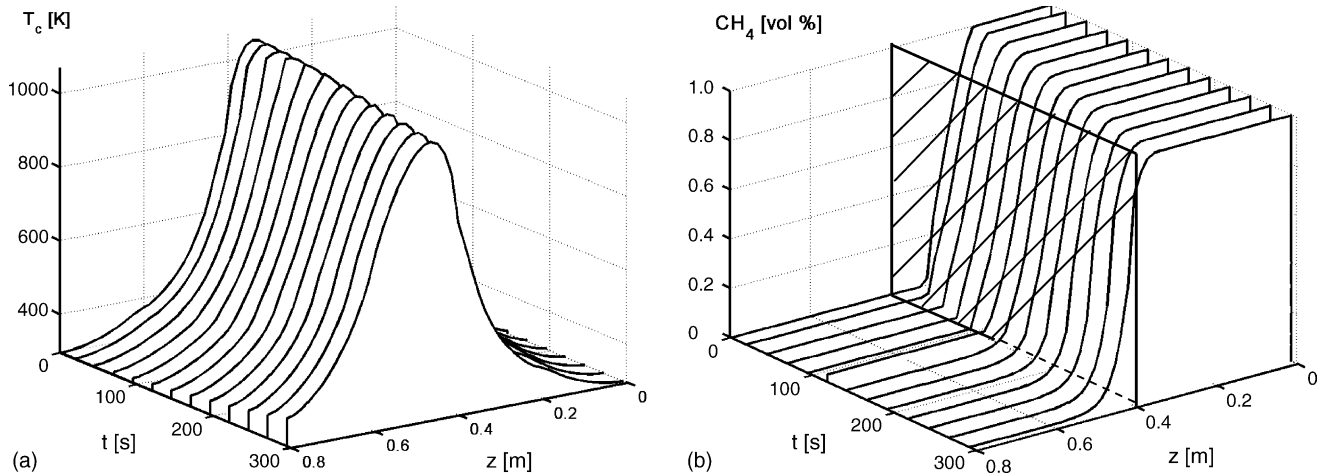


Fig. 6. Reactor bed temperature profiles (a) and corresponding  $\text{CH}_4$  concentration plot (b) in a stable cyclic steady state for 1 vol.% inlet methane concentration and Pd catalyst.

simulation of 100–200 half-cycles of reversal. Fig. 6 presents fairly symmetric cyclic steady-state temperature profiles in the reactor (a) and corresponding concentration plot (b). It is visible from the graph of concentration profiles that close to the end of the reversal half-cycle part of combustion takes place in the second half of the bed, i.e. after the part of gas is withdrawn to the heat recovery boiler.

In Fig. 7 cyclic steady-state temperature profiles along the reactor length, for various inlet concentrations and various hot gas withdrawal flow rates, at the end of the half-cycle are shown, while Fig. 8 presents corresponding methane concentration profiles.

## 5. Summary and conclusions

The results obtained for heat extraction by the hot gas withdrawal (schematic diagram shown in Fig. 1) and man-

ganese catalyst reveal higher temperature within the reactor bed than for palladium catalyst. Consequently,  $\text{MnO}_2$  catalyst practically should not be used due to too high maximum catalyst temperature expected, which could sinter and damage the catalyst. So the higher heat recoveries (above 95%) indicated by the simulations for this type of catalyst may be impossible to attain in practice.

The simulations reveal apparent contradiction between maximum temperature in the reactor and efficiency of the heat recovery. High efficiency of heat recovery can be obtained only on expense of high catalyst temperature. There is a lot of degrees of freedom when designing the process parameters, since one can assume various combinations of inert and catalyst section length, apparent gas velocity in the reactor, size and shape of the catalyst and inert filling, various reversal times and many others. In the case presented the parameters were selected that way to obtain lowest possible

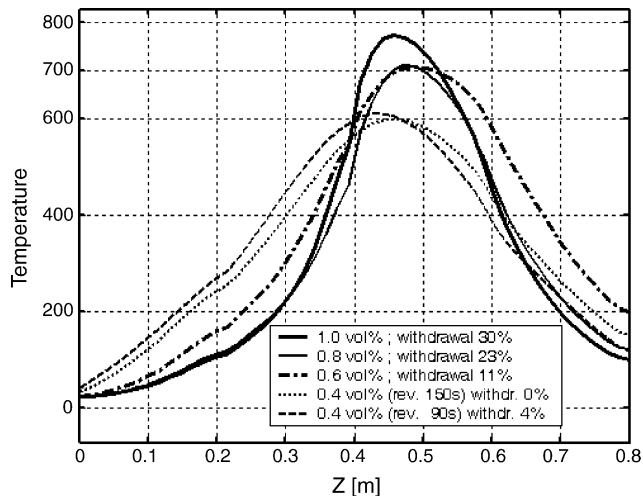


Fig. 7. Cyclic steady-state temperature profiles in the reactor at the end of the reversal half-cycle, for various inlet concentrations and various hot gas withdrawal flow rates.

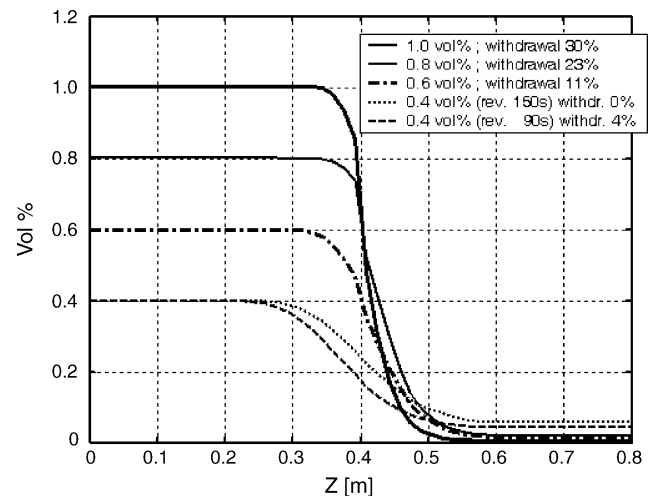


Fig. 8. Cyclic steady-state  $\text{CH}_4$  concentration profiles in the reactor at the end of the half-cycle, for various inlet concentrations and various hot gas withdrawal flow rates.

temperature in the catalyst bed, in order to avoid the catalyst destruction mainly due to appearance of homogeneous combustion in the gas phase. One should be aware, however, that this aim is inconsistent with very high efficiency of the heat recovery.

When heat exchanger is located on the side stream of the hot gas that is then cooled to a preset temperature, which in case of study is assumed 333 K (60 °C), the efficiency of heat recovery will decline with a decrease in the temperature at the inlet to the exchanger. On the one hand, this conclusion seems to be obvious, while hot gas withdrawn is always cooled down to the same target temperature. On the other hand, however, effect of lower inlet temperature to the boiler in the “hot gas withdrawal” system could have been compensated by higher flow rate of the hot gas withdrawn. Unfortunately it occurs that such compensation is not sufficient enough to counterbalance an effect of lower temperature as for higher side stream flow rate the reaction could extinguish. Therefore, for the MnO<sub>2</sub> catalyst which operates at higher temperatures the efficiencies are higher than those for the low-temperature Pd catalyst. Thus, on the one hand, the temperature has to be low enough to protect the catalyst but, on the other, sufficiently high to yield satisfactory efficiencies of the recovery.

For the palladium catalyst the withdrawal up to 30% of the gas leads to a heat recovery coefficient exceeding 70%, i.e., 7 MW per 100,000 m<sup>3</sup>(STP)/h for the feed containing 1 vol.% of methane. If we assume, however, that the heat is produced using ventilation air with an average CH<sub>4</sub> content of 0.5 vol.%, for an average output of a single shaft of about 700,000 m<sup>3</sup>(STP)/h it is possible to recover some 12 MW. For the hot gas withdrawal option the boiler (which is by far the most convenient type of exchanger) would operate at temperatures safeguarding vigorous heat transfer to the various elements of the system (superheaters, evaporators and water heaters). Production of electricity using the heat recovered also seems feasible.

A drawback of the heat recovery through gas withdrawal is a lower conversion of the combustion reaction compared with that for the central cooling option (cf. Fig. 6 from which it can be seen that some conversion occurs past the first half of the bed, i.e., after a portion of the gas has been withdrawn). To solve that problem some quantity of the catalyst can be placed along the path of the side stream withdrawn so that the remaining methane can be further oxidized. This may be a straightforward task as the initial temperature of the extracted stream is usually high enough to provide favourable conditions for the combustion to proceed.

## Acknowledgement

This work was supported by the European Union Grant (Contract No. ICA2-CT-2000-10035).

## References

- [1] Yu.Sh. Matros, *Catalytic Processes under Unsteady Conditions*, Elsevier, Amsterdam, 1989.
- [2] Yu.Sh. Matros, A.S. Noskov, V.A. Chumachenko, O.V. Goldman, Theory and application of unsteady state detoxication of effluent gases from sulfur dioxide, nitrogen oxides and organic compounds, *Chem. Eng. Sci.* 43 (1988) 2061–2066.
- [3] L.L. Gogin, Yu.Sh. Matros, A.G. Ivanov, *Ecology and Catalysis*, Nauka, Novosibirsk, 1990, p. 107.
- [4] H. Sapoundijev, R. Trotter, F. Aube, Heat recovery from lean industrial emissions environmental and economic benefits of CFRR technology, in: *Greenhouse Gas Control Technologies*, Elsevier, 1999, pp. 805–810.
- [5] J. Unger, G. Kolios, G. Eigenberger, On the efficient simulation and analysis of regenerative processes in cyclic operation, *Comput. Chem. Eng.* 21 (1997) 5167–5172.
- [6] K. Gosiewski, Effective approach to cyclic steady state in the catalytic reverse-flow combustion of methane, *Chem. Eng. Sci.* 59 (2004) 4095–4101.
- [7] L.L. Gogin, O.P. Klenov, V.S. Lahmostov, A.S. Noskov, N.A. Chumakova, V.I. Drobyshevich, High parameter heat production in the process of flue gas cleaning, *Chim. Prom.* 12 (1997) 50–56 (in Russian).
- [8] F. Aube, H. Sapoundijev, Mathematical model and numerical simulations of catalytic flow reversal reactors for industrial applications, *Comput. Chem. Eng.* 24 (2000) 2623–2632.
- [9] K. Gosiewski, K. Warmuzinski, Efficient recovery of heat from the catalytic combustion of methane in reverse-flow reactors, *Inżynieria Chemiczna i Procesowa (Chem. Process Eng.)* 23 (2002) 397–413 (in Polish).
- [10] K. Gosiewski, K. Warmuzinski, Efficient heat recovery in the catalytic reverse-flow combustion of methane, in: *Proceedings of the Paper Presented on the IVth International Conference on Unsteady State-Processes in Catalysis (USPC-4)*, Montreal, 2003.
- [11] U. Nowak, J. Frauhammer, U. Nieken, A fully adaptive algorithm for parabolic partial differential equations in one space dimension, *Comput. Chem. Eng.* 20 (1996) 547–561.
- [12] K. Gosiewski, U. Bartmann, M. Moszczyński, L. Mleczko, Effect of the intraparticle mass transport limitations on temperature profiles and catalytic performance of the reverse-flow reactor for the partial oxidation of methane to synthesis gas, *Chem. Eng. Sci.* 54 (1999) 4589–4602.
- [13] EU Project (2001–2003) (Contract No. ICA2-CT-2000-10035), *Methane Recovery – Final Report Part 2*, Boreskov Institute of Catalysis.
- [14] P.G. Tsyrunnikov, V.S. Salnikov, V.A. Drozdov, A.S. Noskov, N.A. Chumakova, V.K. Ermolaev, I.V. Malkhova, Deep oxidation of methane on alumina-manganese and Pt-containing catalysts, *J. Catal.* 198 (2001) 164–171.